J|A|C|S
COMMUNICATIONS

Published on Web 05/14/2008

Origin of Mutational Effects at the C3 and G8 Positions on Hammerhead Ribozyme Catalysis from Molecular Dynamics Simulations

Tai-Sung Lee[†,‡] and Darrin M. York*[,‡]

Consortium for Bioinformatics and Computational Biology, and Department of Chemistry, University of Minnesota, 207 Pleasant Street SE, Minneapolis, Minnesota 55455

Received December 19, 2007; E-mail: york@umn.edu

A detailed understanding of the structure−function relationships in the hammerhead ribozyme[1,2] will aid in the understanding of other cellular RNA catalysts, such as the ribosome, and have potential impact for rational drug design and the development of new biotechnology. Much effort has been devoted to understand the details of the hammerhead ribozyme mechanism both experimentally and theoretically.[1−5] Mutation experiments suggested that two conserved residues, G8 and C3, are critical for catalytic activity.[4] The specific roles of these two residues, however, were not clear from the minimal sequence structures,[6−8] and it was not until the recent full length hammerhead structure[9] was solved that a structural basis emerged that could begin to reconcile these mutational effects and other aspects of the mechanistic debate.

This work reports a series of 10 molecular dynamics simulations of the native and mutated full length hammerhead ribozymes in the reactant state and in an activated precursor state (C17:$O_{2'}$ deprotonated). Mutant simulations include the C3U, G8A, and G8I single mutants and a C3U/G8A double mutant that exhibits an experimental rescue effect.[10] Simulations were performed with NAMD version 2.6[11] using the Cornell et al.[12] all-atom nucleic acid force field (parm94) provided in AMBER9[13] and the TIP3P water model.[14] The initial structure was taken from the 2.0 Å crystal structure[15] with Mn^{2+} ions and solvent resolved (PDB: 2OEU) with Mn^{2+} ions replaced by native Mg^{2+} ions in the simulations. A Mg^{2+} implicated in catalysis was bound to A9:O_{2P} and G10.1:N_7 (Figure 1) in accord with available experimental data.[15,16]

Following 10 ns of ion/solvent equilibration, simulations were performed at 298 K and 1 atm in a cubic cell with PME[17] electrostatics in the presence of ∼11,400 water molecules and 0.14 M NaCl and carried out to 60 ns. Key active site structural parameters are provided in Table 1, and representative hydrogen bond base pairing at the C3−G8 positions is shown in Figure 1. In addition, a set of control simulations were performed on a benign U7C mutation and of the wild type with the active site Mg^{2+} ion removed (see Supporting Information). An assumption herein is that the mutated sequences fold to a native-like structure.

Mg^{2+} can migrate to a bridging position in the activated precursor. In all reactant state simulations, the Mg^{2+} stays near A9:O_{2P} and G10.1:N_7. In all activated precursor state (deprotonated C17:$O_{2'}$) simulations, after a few hundred picoseconds, the Mg^{2+} migrates into a bridging position between A9:O_{2P} and C1.1:O_{2P} and reduces the distance (d_0 in Table 1) by 1 Å relative to the reactant state simulations. The C17:$O_{2'}$ has significant in-line fitness for nucleophilic attack on C1.1:P. In all simulations except G8A, the G8:$O_{2'}$ is hydrogen bonded to the leaving group, C1.1:$O_{5'}$ and positioned to act as the general acid.

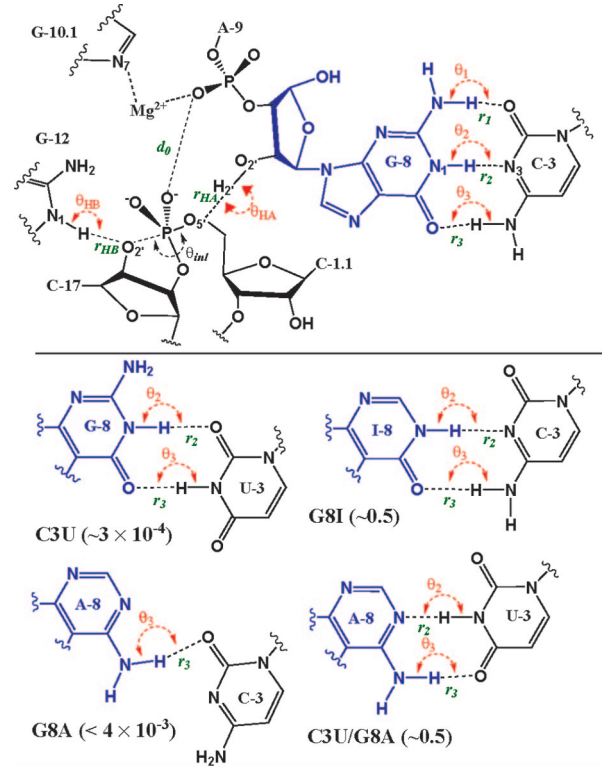

Figure 1. (*Upper*) Active site of the full length hammerhead RNA using the canonical minimal sequence numbering scheme described in refs 6 and 16. (*Lower*) Representative hydrogen bonding of the C3:G8 base pair observed from mutant simulations. Experimental relative catalytic rates of mutant versus wild type minimal sequence ribozymes (k_{mut}/k_{wt}) are shown in parentheses (C3U from ref 18, G8A from ref 19, C3U/G8A from ref 10, and G8I from ref 4) and may differ for the full length sequence.

C3U mutation disrupts the active site in the reactant. The C3U mutation reduces the catalytic rate by a factor ∼3 × 10^{-4}.[18] The C3U mutation disrupts the normal Watson−Crick hydrogen bonding with G8 (Figure 1), causing a base shift that disrupts the active site structure in the reactant state. The distance between the A9 and scissile phosphate increases more than 3.5 Å and breaks key hydrogen bonds between the $O_{2'}$ nucleophile of C17 and N_1 of G12 (the implicated general base) and between the $O_{5'}$ leaving group of C1.1 and $H_{2'}$ of G8 (the implicated general acid). These perturbations in the reactant state would prevent activation of the nucleophile and progress toward the transition state. Experimental evidence shows that C3U indeed reduces the rate constant by more than 3 orders of magnitude.[18]

G8A mutation disrupts the positioning of G8:$O_{2'}$ as general acid in the activated precursor. The G8A mutation reduces the catalytic rate by a factor ≤0.004.[19] Simulation results indicate the G8A

† Consortium for Bioinformatics and Computational Biology.
‡ Department of Chemistry.

10.1021/ja711242b CCC: $40.75

Table 1. Characterization of the Active Site Structure and Fluctuations[a]

	WT	C3U	G8A	C3U/G8A	G8I	d-WT[d]	d-C3U	d-G8A	d-C3U/G8A	d-G8I
d_0	3.98(40)	**7.80(66)**	4.22(34)	3.94(39)	4.27(59)	2.96(12)	2.94(13)	2.95(12)	2.93(12)	2.93(13)
r_{Nu}	3.98(34)	**4.16(14)**	3.2(10)	3.59(48)	3.77(44)	3.54(17)	3.67(16)	3.80(18)	3.62(16)	3.58(18)
θ_{inl}	128.2(116)	127.1(67)	156.0(70)	141.3(169)	131.6(152)	158.6(78)	154.2(74)	146.6(88)	155.5(73)	156.6(73)
r_{NN}[b]	2.97(9)	**3.61(21)**	**5.33(66)**	3.00(19)	2.98(13)	2.96(10)	**3.75(20)**	**6.58(46)**	3.04(15)	2.93(11)
r_{HB}	2.10(26)	**3.51(66)**	2.01(16)	2.38(46)	2.05(26)	2.16(55)	1.94(14)	1.89(12)	1.95(14)	1.99(16)
θ_{HB}	152.1(138)	**121.2(155)**	164.2(85)	147.1(181)	155.6(124)	152.0(151)	155.7(96)	158.5(90)	155.5(93)	156.0(99)
r_{HA}	2.83(44)	**7.82(58)**	2.97(33)	3.27(64)	2.83(86)	2.82(95)	2.99(99)	**4.10(63)**	2.61(91)	2.47(52)
θ_{HA}	118.2(168)	**45.2(164)**	119.3(150)	130.6(198)	118.5(344)	126(398)	108.7(397)	**82.8(215)**	130.6(385)	138.6(286)
%[c]	24.4	**0.0**	31.2	13.2	38.4	62.8	43.6	**0.8**	68.8	77.2

[a] Analysis was performed over the last 25 ns (10 ps sampling). Distance and angles (Figure 1) are in Å and degrees, respectively. Standard deviations (SD) are listed in parentheses divided by the decimal precision of the average. [b] The $N_3 \cdots N_1$ distance between nucleobase in the 3 and 8 position. [c] The hydrogen bond contact percentage of the general acid with the leaving group defined by $r_{HA} \leq 3.0$ Å and $\theta_{HA} \geq 120$ °. [d] The notation "d-" denotes the activated precursor state simulations having the C17:$O_{2'}$ deprotonated.

mutation considerably weakens the base pair with C3 with only one weak hydrogen bond that remains intact (Figure 1). In the reactant state simulation, G8A does not appear to dramatically alter the active site contacts relative to the wild-type simulation, with the exception of the A8:$N_1 \cdots$C3:N_3 distance which increases due to a shift in the hydrogen bond pattern (Figure 1). In the activated precursor state, however, the hydrogen bond positioning between G8:$H_{2'}$ and C1.1:$O_{5'}$ is significantly disrupted relative to the wild-type simulation. The G8A mutation shifts the conserved 2′OH of G8 away from the ideal general acid position and can possibly block the general acid step of the reaction. Mutation of G8 to 2-aminopurine (AP)[4,20] or to 2,6-diaminopurine (diAP),[20] which is expected to have similarly weakened hydrogen bonding as the G8A mutation, reduces the reaction rate by over 3 orders of magnitude.

G8I and C3U/G8A mutations are relatively benign. Whereas the relatively isosteric C3U and G8A mutations lead to considerably reduced catalytic rates, the G8I[4,20] and C3U/G8A[10] mutations affect the rate by less than an order of magnitude. The C3U/G8A double mutation and G8I single mutation simulations indicate that the hydrogen bond network retains the overall base positions relative to the wild-type simulation and suggest that these two mutations do not significantly alter any of the active site indexes that would affect activity relative to the wild-type simulation (Table 1).

Structural deviations that give rise to mutation effects can occur at different stages along the reaction path. Although the canonical Watson−Crick hydrogen bond network is altered significantly in both C3U and G8A mutations, the simulations suggest that the origin of the mutational effect on the ribozyme kinetics can occur at different stages along the reaction path. In the reactant state, the Mg^{2+} ion is bound between the G10.1:N_7 and A9:O_{2P} . The large base pair shift that occurs in the C3U mutation simulation results in a compromise of the active site structure, including the loss of interactions between the proposed general base and nucleophile. In the activated precursor state, the Mg^{2+} ion occupies a bridging position between A9:O_{2P} and the scissile phosphate. The G8A mutation, which is very weakly hydrogen bonded, does not sustain a catalytically viable position of the general acid.

Hydrogen bonding between nucleobases in the 3 and 8 positions is necessary but not sufficient to preserve active site structural integrity. The G8I and C3U/G8A mutations that largely preserve a stable base pair hydrogen bonded scaffold lead to relatively benign mutations. A C3G/G8C base pair switch mutation that preserves hydrogen bonded base pairing partially rescues activity relative to the single mutations, although it still reduces activity 150−200-fold.[9,21] Recent analysis of all base pair mutations indicates considerable variation in activity, but all of the non-native mutations at this position are considerably less active.[21] The present simulation results offer the prediction that, whereas both C3U[18] and G8diAP[20] single mutations are observed experimentally to reduce catalytic activity by several orders of magnitude, a correlated C3U/G8diAP double mutation, which retains base pair hydrogen bonding, should exhibit a partial rescue effect in the hammerhead ribozyme.

Acknowledgment. The authors are grateful for support from the National Institutes of Health, the University of Minnesota Biomedical Informatics and Computational Biology program, the Minnesota Supercomputing Institute (MSI), and generous allocation on the IBM BlueGene at the IBM OnDemand Center in Rochester, Minnesota.

Supporting Information Available: Additional experimental details. This material is available free of charge via the Internet at http://pubs.acs.org.

References

(1) Scott, W. G. *Q. Rev. Biophys.* **1999**, *32*, 241–294.
(2) Scott, W. G. *Curr. Opin. Struct. Biol.* **2007**, *13*, 280–286.
(3) Takagi, Y.; Ikeda, Y.; Taira, K. *Top. Curr. Chem.* **2004**, *232*, 213–251.
(4) Blount, K. F.; Uhlenbeck, O. C. *Annu. Rev. Biophys. Biomol. Struct.* **2005**, *34*, 415–440.
(5) Lee, T.-S.; Silva-Lopez, C.; Martick, M.; Scott, W. G.; York, D. M. *J. Chem. Theory Comput.* **2007**, *3*, 325–327.
(6) Scott, W. G.; Murray, J. B.; Arnold, J. R. P.; Stoddard, B. L.; Klug, A. *Science* **1996**, *274*, 2065–2069.
(7) Murray, J. B.; Terwey, D. P.; Maloney, L.; Karpeisky, A.; Usman, N.; Beigelman, L.; Scott, W. G. *Cell* **1998**, *92*, 665–673.
(8) Murray, J. B.; Szöke, H.; Szöke, A.; Scott, W. G. *Mol. Cell* **2000**, *5*, 279–287.
(9) Martick, M.; Scott, W. G. *Cell* **2006**, *126* (2), 309–320.
(10) Przybilski, R.; Hammann, C. *RNA* **2007**, *13*, 1625–1630.
(11) Phillips, J. C.; Braun, R.; Wang, W.; Gumbart, J.; Tajkhorshid, E.; Villa, E.; Chipot, C.; Skeel, R. D.; Kaleé, L.; Schulten, K. *J. Comput. Chem.* **2005**, *26*, 1781–1802.
(12) Cornell, W. D.; Cieplak, P.; Bayly, C. I.; Gould, I. R.; Ferguson, D. M.; Spellmeyer, D. C.; Fox, T.; Caldwell, J. W.; Kollman, P. A. *J. Am. Chem. Soc.* **1995**, *117*, 5179–5197.
(13) Pearlman, D. A.; Case, D. A.; Caldwell, J. W.; Ross, W. R.; Cheatham, T., III; DeBolt, S.; Ferguson, D.; Seibel, G.; Kollman, P. *Comput. Phys. Commun.* **1995**, *91*, 1–41.
(14) Jorgensen, W. L.; Chandrasekhar, J.; Madura, J. D.; Impey, R. W.; Klein, M. L. *J. Chem. Phys.* **1983**, *79*, 926–935.
(15) Martick, M.; Lee, T.-S.; York, D. M.; Scott, W. G. *Chem. Biol.* **2008**, *15*, 332–342.
(16) Wang, S.; Karbstein, K.; Peracchi, A.; Beigelman, L.; Herschlag, D. *Biochemistry* **1999**, *38*, 14363–14378.
(17) Essmann, U.; Perera, L.; Berkowitz, M. L.; Darden, T.; Hsing, L.; Pedersen, L. G. *J. Chem. Phys.* **1995**, *103*, 8577–8593.
(18) Baidya, N.; Uhlenbeck, O. C. *Biochemistry* **1997**, *36*, 1108–1114.
(19) Ruffner, D. E.; Stormo, G. D.; Uhlenbeck, O. C. *Biochemistry* **1990**, *29*, 10695–10712.
(20) Han, J.; Burke, J. M. *Biochemistry* **2005**, *44*, 7864–7870.
(21) Nelson, J. A.; Uhlenbeck, O. C. *RNA* **2008**, *14*, 43–54.

JA711242B